

The Effect of Dielectric Matrix Electric Field on the Electron Detrapping In ZNS Particles: Modeling and Analysis

SeongMin Kim*

School of Advanced Materials Science and Engineering, Sungkyunkwan University, Suwon 16419, Korea
Corresponding Author: SeongMin Kim

ABSTRACT

The finite element method was used to calculate electric potential within ZnS particles (diameter: $\sim 30 \mu\text{m}$) surrounded by a dielectric matrix with various charges. The dielectric matrix used in the simulation is nylon, polydimethylsiloxane (PDMS), polymethyl methacrylate (PMMA), polyimide (PI), polyethylene, polytetrafluoroethylene (PTFE), polyvinyl chloride (PVC), PVDF_10 (polyvinylidene fluoride) and PVDF_50. As a result, the trapped electrons of ZnS in the PTFE dielectric matrix can be more freely moved to the conduction band, assuming that the PTFE has the highest potential gradient that can detrapp electrons better at shallow trap levels among other dielectric matrices.

Keywords: dielectric matrix, electric field, detrapping, ZnS particle

Date of Submission: 13-10-2017

Date of Publication: 27-10-2017

I. INTRODUCTION

ZnS phosphor doped with Cu or Mn can be excited by an electric field called EL (electroluminescence) [1-5] or a stress called piezoluminescence [6-10], which emits light. Such luminescence is associated with body radiation stimulated by the external electric field [1-5] or mechanical stress [6-10]. Many applications using these two types of stimuli have been used for visualized sensing [11] or pressure mapping [12]. Here we have calculated the electric potential of ZnS particles of about $30 \mu\text{m}$ diameter inserted into various dielectric matrices in the presence of an external electric field. Detrapping is related to the slope of the conduction and valence band (i.e., band bending) of ZnS where the electrons trapped at the sulfur vacancies can be transported to the conduction band. The charged dielectric matrix is modeled by applying equal and opposite surface charges to the top and bottom boundaries, which in turn induces an external electric field through the ZnS particles as shown in Figure 1. The dielectric matrix used for numerical simulations using the finite element method (COMSOL software package) is as follows: Nylon, PDMS (Polydimethylsiloxane), PMMA (Polymethyl methacrylate), PI (Polyimide), Polyethylene, PTFE (Polytetrafluoroethylene), PVC (Polyvinyl chloride), PVDF_10 (Polyvinylidene fluoride), and PVDF_50. As a result, the PTFE matrix has been found to have the highest potential gradients that can be used to design and control field-induced emission for impurity doped ZnS.

II. RESULTS AND DISCUSSION

Since the ZnS particles can be doped with an impurity such as Cu or Mn, the trapped electrons below the conduction band can be falling to the impurity level, emitting light. This luminescence mechanism is related to the detrapping of electrons at the trap level and the intensity is related to how well the electrons are detrapped. Detrapping is easier if the trap level is close to the conduction band. Otherwise, it is difficult for the electrons to be detrapped at deep levels. When an external electric field is induced around the ZnS particles, tilt of the conduction and the valence band occur, and the trap site approaches the conduction band. (Easy way to detrapping for electrons)

The external electric field can be controlled by various types of matrices due to their different dielectric constants. To model the mechanism of this system, ZnS particles are embedded in various dielectric matrices. To compare the dielectric effects for them, the same external field must be created by placing the same and opposite charge on the upper and lower bounds (in this case the direction of the electric field is formed from top to bottom). Figure 2 shows a 3D simulation of the electric potential distribution along the diameter of the ZnS particles (① to ②) inside the charged matrix with different dielectric constants. As a result, small dielectric constants follow in order: PTFE, polyethylene, PDMS, PMMA, PVC, polyimide, nylon, PVDF_10 and PVDF_50.

The reason why the electric potential of ZnS decreases with the increase of the matrix dielectric constant, ϵ can be understood in this way. The problem is reduced to the dielectric sphere in the dielectric field. A uniform electric field is generated by equal and opposite charge away from the ZnS sphere. This field is

represented by $\vec{E} = E_0 \hat{k}$ corresponding to the potential of $\varphi = -E_0 r \cos \theta$. Potential can be expanded in terms of Legendre polynomials both inside and outside the area.

$$\varphi_{in}(r, \theta) = A_2 r \cos \theta \quad \dots\dots\dots (1)$$

$$\varphi_{out}(r, \theta) = A_1 r \cos \theta + \frac{B_1}{r^2} \cos \theta \quad \dots\dots\dots (2)$$

As far as the asymptotic limit,

$$A_1 = -E_0 \quad \dots\dots\dots (3)$$

The electric potential should be continuous at $r = R$ (spherical surface)

$$-E_0 R + \frac{B_1}{R^2} = A_2 \cdot R \quad \dots\dots\dots (4)$$

Sphere boundary conditions free of charge are used

$$-\epsilon_{ZnS} \frac{\partial \varphi_{in}}{\partial r} \Big|_{r=R} = -\epsilon \frac{\partial \varphi_{out}}{\partial r} \Big|_{r=R} \quad \dots\dots\dots (5)$$

$$-\epsilon_{ZnS} \cdot A_2 = \epsilon E_0 + \epsilon \frac{2B_1}{R^3} \quad \dots\dots\dots (6)$$

Therefore, the coefficient B_1 and A_2 can be obtained

$$B_1 = E_0 R^3 \left(\frac{\epsilon - \epsilon_{ZnS}}{\epsilon_{ZnS} + 2\epsilon} \right) \quad \dots\dots\dots (7)$$

$$A_2 = -\frac{3E_0}{\frac{\epsilon}{\epsilon_{ZnS}} + 2} \quad \dots\dots\dots (8)$$

So that the electric potential inside the ZnS is

$$\varphi_{in} = \left(\frac{-3E_0}{\frac{\epsilon}{\epsilon_{ZnS}} + 2} \right) r \cos \theta \quad \dots\dots\dots (9)$$

According to Eq (9), φ_{in} is inversely proportional to the dielectric constant of the matrix, ϵ . If ϵ increases, φ_{in} decreases as shown in Fig. 2.

A cross section of the potential gradient of the ZnS particles embedded in the various matrices is shown in Figure 3. As the dielectric constant of the matrix increases, the potential gradient disappears. Based on these numerical results, we can design an electronic detrapping process. Because the electrons trapped in the sulfur vacancies, Vs can be easily detrapped due to the potential gradient, the intensity of the dielectric matrix electric field is an important factor affecting the detrapping of electrons. The higher the slope of the potential, the shorter the trap distance from the conduction band as shown in Fig. 4. In our case, the PTFE matrix has the highest gradient of electric potential, which means that it is much easier to detrapp electrons compared with the others.

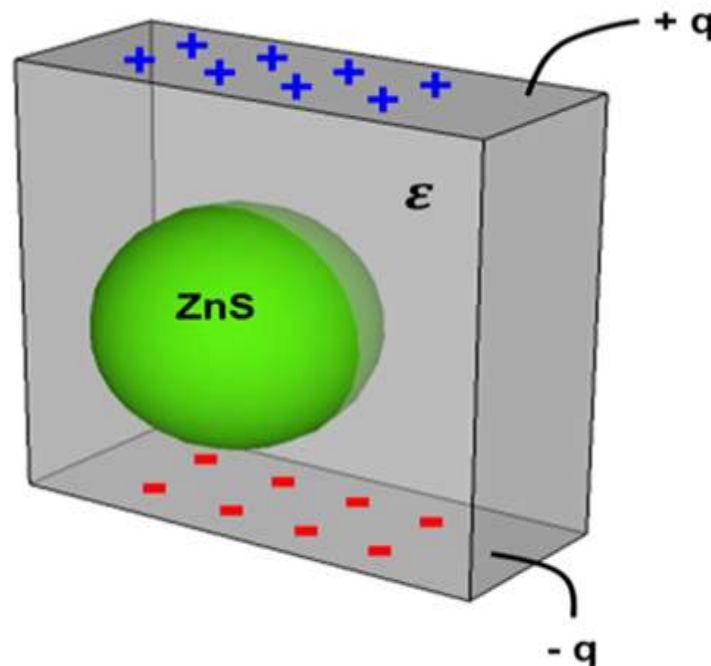


Figure 1: Schematic of ZnS particles placed in a dielectric matrix (ϵ). The external field is built by equal and opposite charge, $q, -q$.

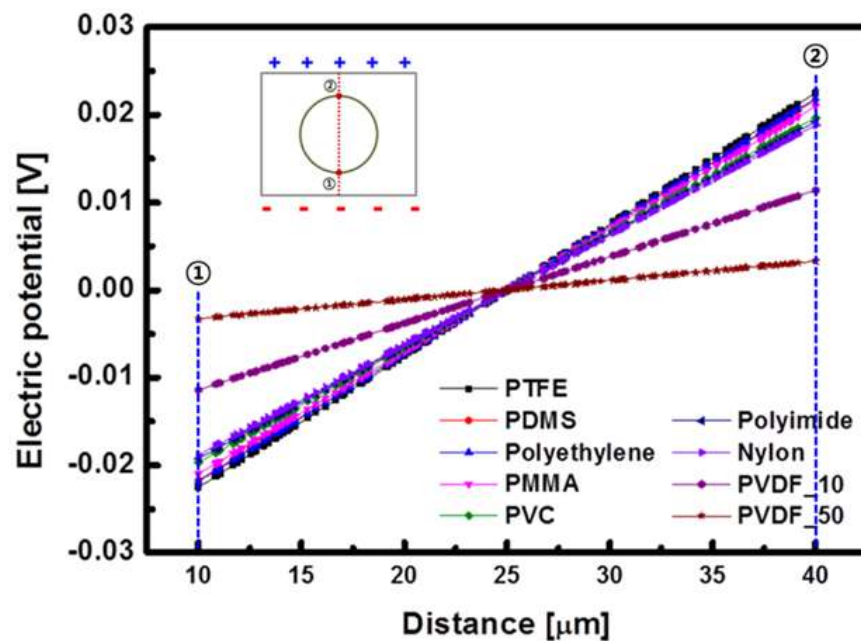


Figure 2: A plot of the electric potentials of the ZnS particles by the nine different dielectric matrices vs. distance from ① to ② (shown in the inset). The circle represents ZnS particles in the charged matrix. PTFE shows the highest slope of the potential along the diameter of the ZnS particles.

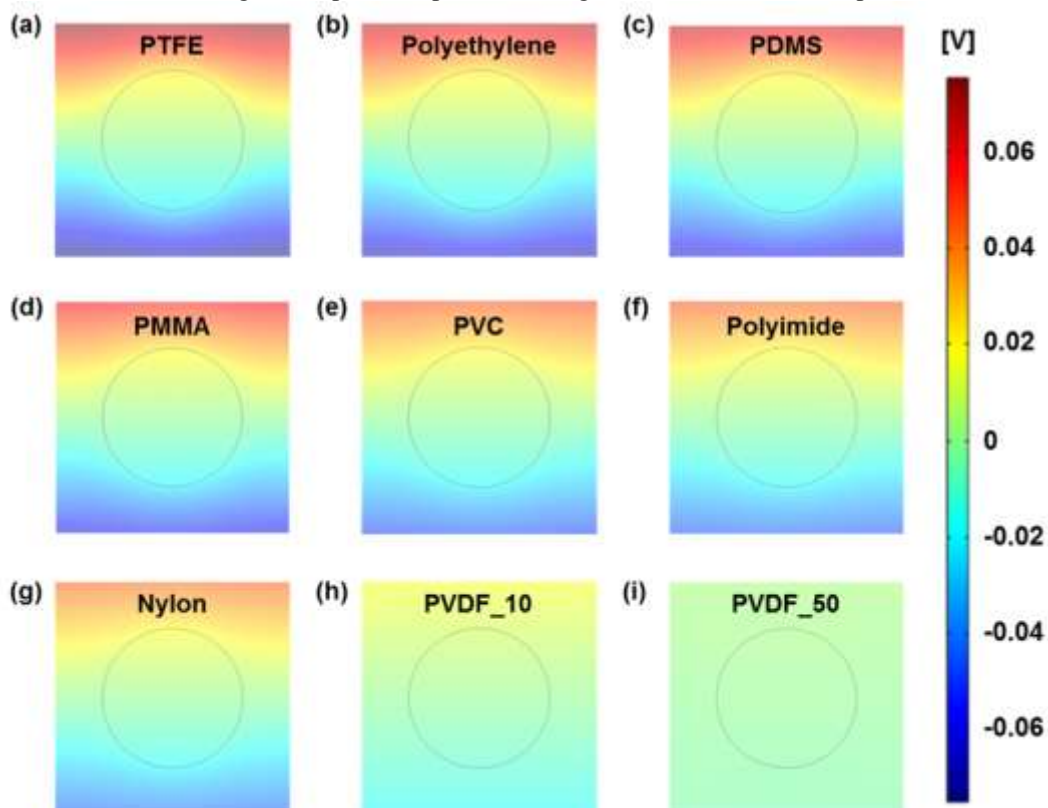


Figure 3: Cross-sectional images of electric potential using various dielectric matrices: (a) PTFE, (b) Polyethylene, (c) PDMS, (d) PMMA, (e) PVC, (f) Polyimide, (g) Nylon, (h) PVDF₁₀, and (i) PVDF₅₀. The number of PVDF indicates a dielectric constant.

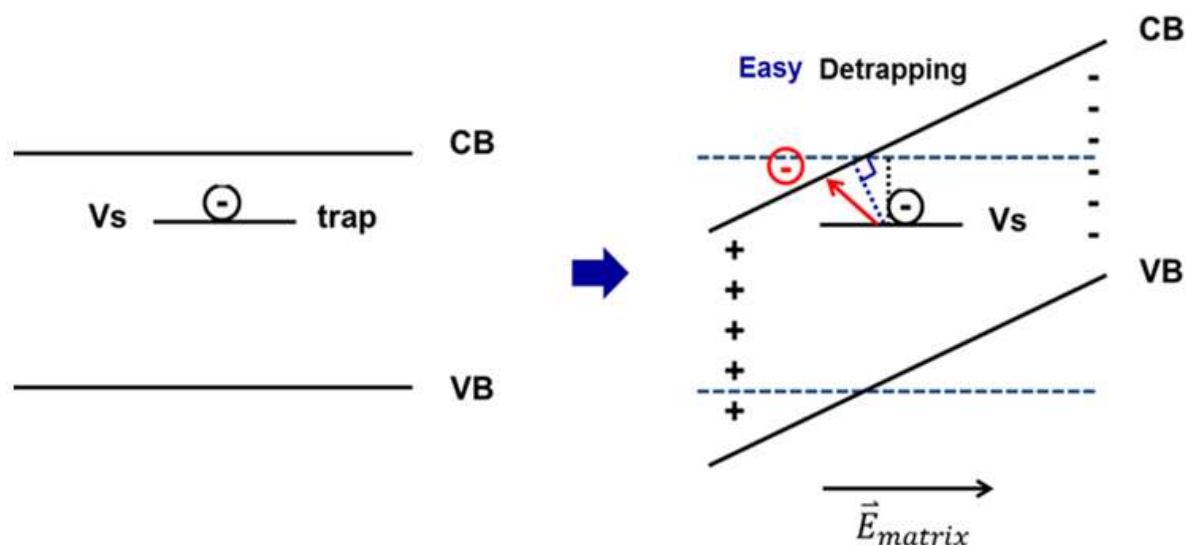


Figure 4: Schematic diagram of conduction and valence band bending by dielectric matrix electric field. Electrons can be detrapped by this field from the trap site (V_s : sulfur vacancy)

III. CONCLUSION

ZnS particles, commonly used as phosphors embedded in various dielectric matrices, are simulated to see their effect on the potential by the matrix field. A total of nine different matrices are used: Nylon, PDMS, PMMA, PI, Polyethylene, PTFE, PVC, PVDF_10, and PVDF_50. According to the simulation, PTFE has been found to theoretically primarily affect band gradients, which can help eliminate electrons from sulfur vacancies. Therefore, this paper can be used to design the detrapping process of phosphor particles in luminescence applications.

ACKNOWLEDGMENTS

This work is supported by the mathematical modeling & analysis group in Korea (NRF-2017R1A2B4010642), and I would like to thank J. Ha for his help.

REFERENCES

- [1]. Elias TA: Homogeneously bright, flexible, and foldable lighting devices with functionalized graphene electrodes. *ACS Appl Mater Interfaces* 2016;8: 16541–16545.
- [2]. Larson C: Highly stretchable electroluminescent skin for optical signaling and tactile sensing, *Science*. 2016;351: 1071-1074.
- [3]. Jinwoo S: AC field-induced polymer electroluminescence with single wall carbon nanotubes. *Nano Lett.* 2011;11: 966–972.
- [4]. Michael B: Materials for powder-based AC-electroluminescence. *Materials* 2010;3: 1353-1374.
- [5]. Flurin S: Bright stretchable alternating current electroluminescent displays based on high permittivity composites *Adv Mater.* 2016;28: 7200–7203.
- [6]. Jiayong G: Enhanced piezoluminescence in non-stoichiometric ZnS:Cumicroparticle based light emitting elastomers, *J Mater Chem C* 2017;5: 5387-5394.
- [7]. Reynolds GT: Piezoluminescence from a ferroelectric polymer and quartz. *JOL.* 1997;75: 295-299.
- [8]. Chao-Nan X: Novel approach to dynamic imaging of stress distribution with piezoluminescence, *Ferroelectrics* 2001;263: 3-8.
- [9]. Ariga K: Piezoluminescence based on molecular recognition by dynamic cavity array of steroid cyclophanes at the air– water interface. *J Am Chem Soc.* 2000;122: 7835–7836.
- [10]. Kohmoto S: Piezoluminescence and liquid crystallinity of 4, 4'-(9, 10-Anthracenediyl) bispyridinium salts. *Cryst Growth Des.* 2015;15: 2723–2731.
- [11]. Xiao YW: Dynamic triboelectrification-induced electroluminescence and its use in visualized sensing, *Adv Mater.* 2016;28: 6656-6664.
- [12]. Xiandi W: Dynamic pressure mapping of personalized handwriting by a flexible sensor matrix based on the mechanoluminescence process. *Adv. Mater.* 2015;27: 2324-2331.